18. M. Madon and J.-P. Poirier, *Phys. Earth Planet. Inter.* **33**, 31 (1983).
19. G. D. Price, *ibid.*, p. 137.
20. P. J. Vaughan and D. L. Kohlstedt, *Phys. Chem. Miner.* **7**, 241 (1981).
21. A. J. Brearley, D. C. Rubie, E. Ito, *ibid.* **18**, 343 (1992).
22. D. C. Rubie, in *MAC Short Course on Experiments at High Pressure and Applications to the Earth's Mantle*, R. W. Luth, Ed. (Mineralogical Association of Canada, Edmonton, 1993), vol. 21, p. 247.
23. The pressure assembly for the experiments was a MgO octahedron, with a 10-mm edge length, containing a $LaCrO_3$ heater (D. Canil, *Phys. Earth Planet. Inter.*, in press). It was compressed with Toshiba F-grade WC anvils with 5-mm truncations. Sample pressure was calibrated at 1200°C by reversing phase transitions in SiO_2 (quartz-coesite and coesite-stishovite) and Mg_2SiO_4 (α-β and β-γ). The uncertainty in the quoted pressures is ±1 GPa. Temperature was monitored with a W3%Re-W25%Re thermocouple without correction for the effect of pressure on the thermocouple. The Mg_2SiO_4 samples were contained in 1.6-mm-diameter Pt capsules, and before the experiments, samples were dried for several hours at 230°C in a vacuum oven.
24. Doubly polished petrographic thin sections suitable for TEM studies were prepared from the experimental charges. Selected areas of the sample were demounted from the thin section and prepared for TEM examination by conventional ion beam milling. After carbon coating, all the samples were studied in a JEOL 2000FX analytical transmission electron microscope operating at 200 kV.
25. Ideally, the synthesis of the γ-Mg_2SiO_4 starting material and the subsequent partial transformation to β would have been accomplished in a single experiment, as described for the β to γ transformation. This procedure was not adopted because it would have involved reducing the sample pressure during the experiment; the sample pressure during decompression in the multi-anvil apparatus has not been calibrated, and it is unlikely that this could be done reliably. Pressurizing the γ-Mg_2SiO_4 at high temperature to reach the β stability field (as was done for the β to γ transformation) would have risked transformation of the sample into forsterite during compression through the α-Mg_2SiO_4 stability field.
26. A. J. Brearley and D. C. Rubie, *Phys. Earth Planet. Inter*, in press.
27. G. W. Groves and A. Kelly, *Philos. Mag.* **8**, 877 (1963).
28. M. Akoagi, E. Ito, A. Navrotsky, *J. Geophys. Res.* **94**, 15671 (1989).
29. D. C. Rubie, T. G. Sharp, A. Hofgrefe, F. Seifert, *Eos* **74**, 93 (1993).
30. E. Ito and T. Katsura, *Geophys. Res. Lett.* **16**, 425 (1989).
31. We are grateful to H. W. Green II and an anonymous reviewer for their constructive reviews and C. R. Ross II for determining the number of independent slip systems that can cause shear transformation in γ-Mg_2SiO_4. We thank H. Schulze for preparing the thin sections and H. Küfner and G. Herrmannsdörfer for technical assistance with the high-pressure experiments. Electron microscopy was carried out in the Electron Microbeam Analysis Facility, Department of Earth Sciences and Institute of Meteoritics, University of New Mexico. Partial funding was provided by National Science Foundation grant EAR 9104777 (A.J.B.).

18 January 1994; accepted 11 April 1994

Arabidopsis ABA Response Gene *ABI1*: Features of a Calcium-Modulated Protein Phosphatase

Jeffrey Leung, Michelle Bouvier-Durand, Peter-Christian Morris, Danièle Guerrier, Françoise Chefdor, Jérôme Giraudat*

The *Arabidopsis ABI1* locus is essential for a wide spectrum of abscisic acid (ABA) responses throughout plant development. Here, *ABI1* was shown to regulate stomatal aperture in leaves and mitotic activity in root meristems. The *ABI1* gene was cloned and predicted to encode a signaling protein. Although its carboxyl-terminal domain is related to serine-threonine phosphatase 2C, the ABI1 protein has a unique amino-terminal extension containing an EF hand calcium-binding site. These results suggest that the ABI1 protein is a Ca^{2+}-modulated phosphatase and functions to integrate ABA and Ca^{2+} signals with phosphorylation-dependent response pathways.

The plant hormone ABA regulates diverse physiological processes including seed maturation and dormancy, as well as the adaptation of vegetative tissues to environmental stresses (*1*, *2*). The responses of this hormone range from the rapid alteration of ion fluxes in stomata (*3*) to the induction of specific changes in gene expression (*1*, *4*). However, the knowledge of the molecular network that couples ABA perception to an integrated set of physiological responses remains fragmentary. Several ABA-regulated genes (*4*) and corresponding transcription factors (*5*) have been identified. Saturable ABA-binding sites have also been reported (*6*), but these proteins have not been further characterized. On the other hand, ABA response mutants offer a propitious means to isolate signaling elements and, furthermore, provide insight into their biological functions on the basis of their associated mutant phenotypes. This approach has led to the cloning of the maize *VP1* (*7*) and *Arabidopsis ABI3* (*8*) loci, whose molecular actions appear to target seed-specific developmental processes. Critical to our understanding of the early events in hormone perception and transduction, however, are probably mutants that exhibit pleiotropic phenotypes. In this regard, mutations in the *Arabidopsis* abscisic acid insensitive 1 (*ABI1*) gene (*9*) appear to have unraveled such an early signaling component. The *abi1* mutations severely impair a wide spectrum of ABA responses including reduced seed dormancy, excessive water loss, and abnormal drought rhizogenesis (*9*, *10*). Moreover, the expression of several ABA- or stress-induced genes has been found to be greatly diminished in the mutants (*11*). To elucidate the regulatory role of the *ABI1* gene product in these diverse developmental, tissue-specific, and adaptive response pathways, we cloned the locus by chromosome walking.

As an aid to localize the gene by plant transformation and to interpret the molecular function of the protein later, we first analyzed two phenotypic traits of the *abi1-1* mutant. One characteristic phenotype of *abi1-1* mutant (*9*) seedlings is their ability to achieve root development in the presence of inhibitory concentrations of applied ABA (Fig. 1, A and B). Indeed, *abi1-1* root meristems exhibited active cell division in the presence of added ABA, as revealed by the nuclear incorporation of bromodeoxyuridine (BrdU) (*12*), which traces passage through the S phase of the mitotic cycle (Fig. 1, D and F), and the observation of occasional mitotic figures (*13*). In contrast, no BrdU incorporation was detectable in the wild type treated with ABA (Fig. 1, C and E). These results indicate the involvement of the *ABI1* gene product in mediating the ABA inhibition of mitotic activity in the root meristem. Another trait of the *abi1-1* mutant is that the mean aperture of the stomatal pores present on the abaxial (lower) surface of freshly detached rosette leaves in *abi1-1* (8.6 ± 3.3 μm, $n = 115$) is twice as large as that in the wild type (4.1 ± 2.1 μm, $n = 110$) (*14*) (Fig. 1, G and H). Altered stomatal regulation is consistent with the wilty phenotype displayed by the *abi1-1* mutant (*9*).

To clone the *ABI1* locus, restriction fragment length polymorphism (RFLP) linkage analysis was used to delineate a small genomic region that contains the target gene. Plants selected for recombination between *abi1-1* and flanking morphological markers *cer2* and *cer4* on chromosome 4 were used to analyze the linkage of the *abi1-1* mutation with existing RFLP markers assigned to this region (*15*). One of these (PG11), found to map about 0.5 to 1.0 centimorgan from the *ABI1* locus and to represent the closest available RFLP marker (*16*), was used to initiate a chromosome walk. Genomic clones identified from two yeast artificial chromosome (YAC) libraries of *Arabidopsis* (*17*) were used to assemble in successive steps an overlapping set of 13 YACs extending approximately

Institut des Sciences Végétales, Centre National de la Recherche Scientifique UPR 40, Avenue de la Terrasse, 91198 Gif-sur-Yvette Cedex, France.

*To whom correspondence should be addressed.

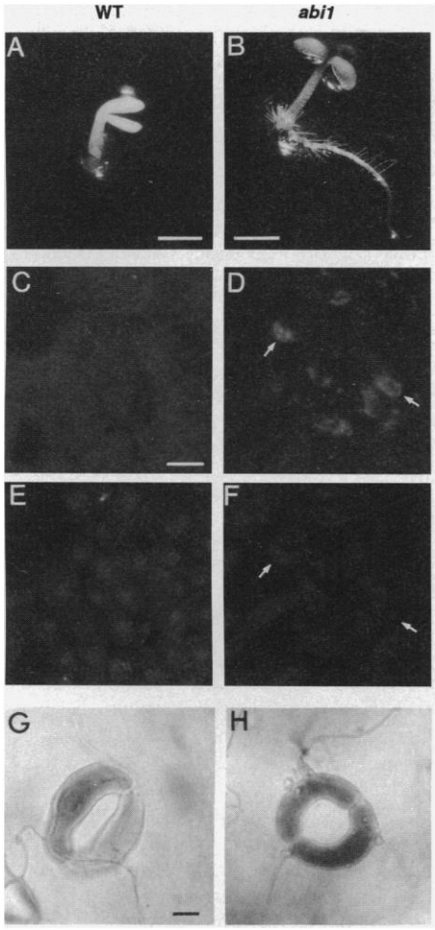

Fig. 1. Characterization of two distinctive traits of the *abi1-1* mutant. The earliest (as soon as 2 days after germination) detectable difference between wild-type (WT) and *abi1* seedlings is the ability of the mutant root to develop and to grow into ABA-containing medium. Photographs show (**A**) wild-type Landsberg (Lan) and (**B**) *abi1-1* seedlings germinated and grown for 6 days in the presence of 10 μM ABA (*12*). Photomicrographs of squashed root meristematic zones derived from such 6-day-old ABA-treated (**C** and **E**) wild-type and (**D** and **F**) *abi1-1* seedlings are shown. The incorporation of BrdU was monitored with a monoclonal antibody to BrdU and secondary antibodies conjugated to fluorescein isothiocyanate (FITC) (C and D). In the same fields, nuclei were revealed by propidium iodide (PI) staining of DNA (E and F). Only background FITC fluorescence was detected in the wild-type nuclei (C), whereas BrdU incorporation was observed in 10 to 20% (depending on the samples) of the *abi1-1* nuclei (D). To facilitate alignment of FITC and PI signals, two *abi1-1* nuclei with incorporated BrdU are indicated by arrows in (D) and (F), respectively. Similar BrdU incorporation was observed in rootlets of wild-type and *abi1-1* seedlings grown without ABA, and no FITC-fluorescence signal was detected in controls where incubation with the primary anti-BrdU antibody was omitted. Photomicrographs of (**G**) wild-type and (**H**) *abi1-1* stomata from the abaxial surface of rosette leaves (*14*). Bars represent (A) 0.5 mm, (B) 1 mm, (C to F) 20 μm, or (G and H) 10 μm.

500 kb toward *ABI1* (*18*) (Fig. 2A). The position of the *ABI1* locus within this "contig" was progressively delimited to a maximal segment of 150 kb by RFLP linkage analysis with the use of probes specific for the ends of overlapping YACs and subsequently with overlapping cosmid subclones derived from YACs EW3H7 and EW11E4 (Fig. 2A).

The *abi1-1* mutation is dominant over the wild-type *ABI1* allele (*9*), even when the mutation is maintained in a triploid genetic background (*19*). This dominance indicates that the *abi1-1* gene could be functionally identified by the transformation of mutant DNA into wild-type plants. To achieve this transformation, we have re-isolated the above 150-kb genomic segment from the *abi1-1* mutant as a set of overlapping phage clones. The inserts from eight of these phages, covering about 90 kb of the region surveyed (Fig. 2A), were then individually subcloned into a transferred DNA (T-DNA) vector and introduced (*20*) into wild-type *Arabidopsis* line C24 (*21*). One clone, λE4-1R2, induced the phenotype of ABA-resistant root growth, which segregated among the progeny (T1) derived from 17 of the 20 independent primary (T0) transformants (Fig. 3A). These transgenic T1 plants also had an increased tendency to wilt during propagation in the greenhouse. Furthermore, seven of these lines were more severe in this phenotype

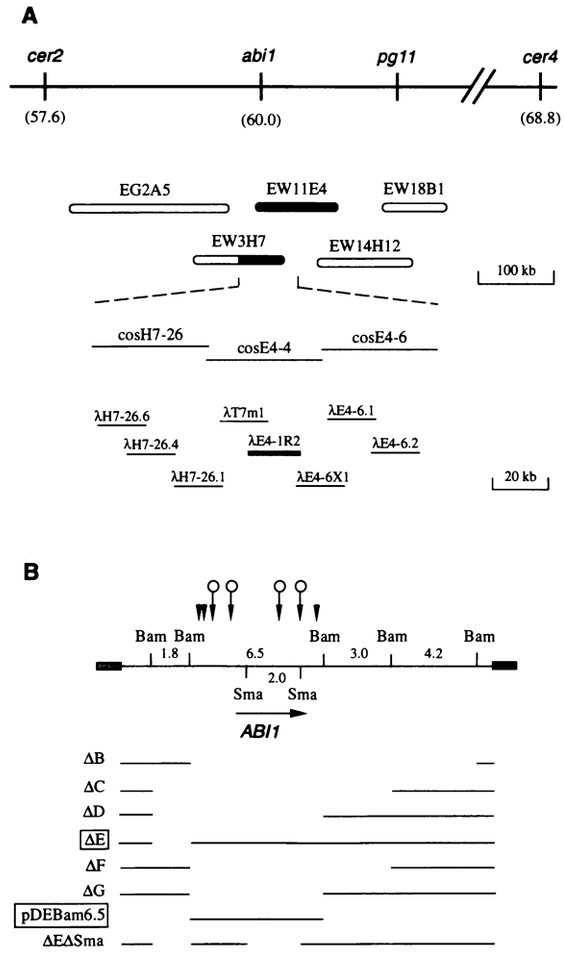

Fig. 2. Map-based cloning of the *ABI1* gene. (**A**) Summary of the chromosome walk. The genetic positions (*15*) of *cer2*, *abi1*, and *cer4* are indicated. RFLP marker PG11 was used as the starting point for chromosome walking, and 13 overlapping YACs were identified (*18*). The five YACs schematically depicted here provide the most faithful representation of the corresponding *Arabidopsis* genomic region as judged from comparative Southern blotting analysis between *Arabidopsis* genomic and YAC DNA. The target gene was limited by RFLP analysis (*16*) to within a 150-kb segment (indicated in black) represented by YACs EW3H7 and EW11E4. This segment was subcloned as cosmids, and 50 of these cosmid clones were ordered into a contig by standard restriction mapping and Southern blotting. Some of these were used in turn to screen a λ genomic library constructed with DNA isolated from *abi1-1*, and a set of 30 overlapping λ clones was then used to reassemble a similar 150-kb contig. Subclones of YACs propagated in cosmid *cos*Pneo and the *abi1-1* genomic library in phage λFIXII (Stratagene) were constructed essentially as described (*37*). Only three of these wild-type cosmids and eight of the *abi1-1* λ clones spanning about 90 kb around the target locus are shown. The clone λE4-1R2, which conferred the mutant phenotypes expected for *abi1* in transgenic plants (Fig. 3), is indicated by the bold line. (**B**) Constructs used to localize the *abi1* locus in the insert of λE4-1R2 by plant transformation. A map of the insert in λE4-1R2, displaying only the restriction sites for Bam HI (Bam) and Sma I (Sma), is shown (sizes in kilobases). A series of constructs bearing internal deletions was generated (*22*). The structure of their DNA inserts is depicted with lines, and those constructs (ΔE and pDEBam6.5) found to induce ABA-resistant root growth are boxed. Deletion of the internal 2.0-kb Sma I fragment (ΔEΔSma) disrupts the ability of the ΔE construct to induce this phenotype. Derivatives of the ΔE construct carrying Tn5 transposons inserted into the 6.5-kb region are shown as arrowheads; those that destroyed the transgene's ability to induce the mutant phenotype are marked with attached circles. The position of the *ABI1* cDNA is shown below the restriction map with the arrow indicating the direction of transcription from 5′ to 3′.

than the original *abi1-1* mutant, because they were almost completely sterile as a result of premature silique desiccation. In addition, T2 seed progeny homozygous for the λE4-1R2 transgene (in all three randomly selected lines tested) showed reduced seed dormancy (9) (Fig. 3B). The observation that these three *abi1-1* characteristic phenotypes co-segregated with the transformed λE4-1R2 fragment indicated that the *abi1-1* gene was within this phage insert (~18 kb).

We focused on ABA-resistant root growth as the most convenient criterion by which to localize further the gene in λE4-1R2. Deletion constructs (ΔB to ΔG) and an internal fragment (pDEBam6.5) derived from this phage (*22*) were functionally tested (Fig. 2B). The results of this testing allowed us to delimit initially the mutant gene within the 6.5-kb Bam HI fragment represented by pDEBam6.5. By using this fragment as a probe to screen complementary DNA (cDNA) banks constructed with mRNA isolated from either leaves or siliques of *Arabidopsis* plants (a total of ~2.0 × 10^6 plaques screened), we recovered a single class of cDNA (25 clones) that mapped entirely within this 6.5-kb Bam HI fragment (Fig. 2B). One of these cDNAs (pcABI1-C38) was nearly full length and was characterized further. Altering the corresponding gene (transcribed or putative promoter regions) either by deletion (ΔEΔSma) or by Tn5 insertion mutagenesis (*22*) led to the complete loss of the transgene's ability to induce the ABA resistance phenotype (Fig. 2B). These targeted gene disruptions prove that the *ABI1* gene has been identified.

Upon RNA blot analysis (*23*), the clone pcABI1-C38 detected a single ~2.0-kb *ABI1* transcript expressed in all of the wild-type tissues examined (roots, leaves, stems, and green siliques). Plantlets of the *abi1-1* mutant allele had similar levels of this transcript as the wild type. On the basis of the determination of the cDNA (pcABI1-C38) and genomic nucleotide sequences (*24*), the *ABI1* gene contains four exons (Fig. 4A) encoding a protein of 434 amino acids with a calculated molecular mass of 47.5 kD and an isoelectric point of 6.02.

The *ABI1* gene product predicts a novel type of signaling enzyme in that the amino-terminal portion displays no extensive similarity with available protein sequences (*25*). However, it is marked locally with all of the structural elements for a type of calcium-binding site known as the EF hand (*26*). Amino acid residues 93 to 104 of the *ABI1* protein fit the consensus sequence (*27*) for the calcium-binding fold of the EF hand and are further flanked on both sides by segments (residues 80 to 90 and 104 to 114) with predicted α-helical conformation (*28*) (Fig. 4B).

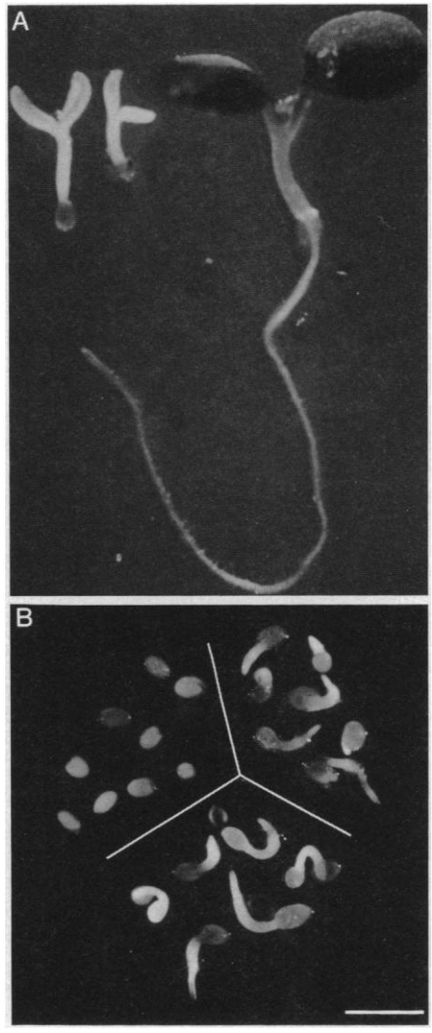

Fig. 3. Functional identification of the *abi1-1* mutant gene in transgenic plants. (**A**) Seedlings of *Arabidopsis* germinated and grown in the presence of 3 μM ABA for 1 week. Root development is impaired in (left) the wild-type C24 seedlings but not in (right) the C24 transgenic seedling harboring the *abi1-1* DNA insert of λE4-1R2. This difference represents the primary criterion used to discriminate between constructs containing and not containing the functional *abi1-1* gene (*36*). A lower concentration of ABA was used here than in experiments described in Fig. 1 to avoid the selection of exclusively "high"-expressing transgenic lines; nevertheless, the Lan wild-type and original *abi1-1* mutant exhibited the same differential root growth on either ABA concentration. (**B**) Freshly harvested mature *Arabidopsis* seeds germinated for 2 days on ABA-free medium. As with the original Lan *abi1-1* mutant (upper right), seeds of a C24 transgenic plant homozygous for the λE4-1R2 construct (bottom) displayed reduced dormancy because they germinated early and synchronously, as compared to wild-type C24 (upper left) and Lan (*36*). The bar represents 1 mm (A and B).

On the other hand, the carboxyl-terminal domain of the predicted ABI1 protein has substantial sequence similarity (55% similarity, 35% identity) with the 2C class of serine-threonine protein phosphatases (PP2Cs) identified in rat (*29*) and yeast (*30*) (Fig. 4B). The same level of sequence similarity (57% similarity, 36% identity) is observed between the rat and yeast enzymes, for which characteristic PP2C activity has been documented. In the case of the *abi1-1* mutant, we have identified a single nucleotide substitution that converts Gly^{180} to Asp. Although Ala residues are found at the coincidental position in both rat and yeast PP2Cs, ABI1 Gly^{180} is embedded in a sizable block of contiguous sequence identities with PP2Cs (Fig. 4B). This block of conserved amino acids is probably functionally important because the *abi1-1* nucleotide change leads to gain-of-function mutant phenotypes (*19*). Both the negative charge and the higher steric hindrance of the *abi1-1* Asp^{180} side chain are likely to alter the properties of the ABI1 carboxyl-terminal domain and might, for instance, lead to constitutive phosphatase activity, altered substrate affinity, or specificity.

This combination of an EF hand motif and a PP2C-like domain in the ABI1 protein is striking because classical PP2Cs are all dependent on Mg^{2+} or Mn^{2+}, but not Ca^{2+}, for enzymatic activity (*29–31*). Also, the only Ca^{2+}-dependent serine-threonine phosphatases known so far are the calcineurins (or PP2Bs) that, unlike ABI1, are heterodimeric proteins composed of a regulatory subunit with EF hands and a distinct catalytic subunit that has no sequence similarity to PP2Cs (*31*).

The primary structure of the ABI1 protein suggests that it is a calcium-modulated phosphatase. The direct involvement of the wild-type protein in ABA signaling would still need to be clarified by, for instance, the isolation and characterization of loss-of-function alleles of *ABI1*. However, the features of the ABI1 protein raise attractive possibilities regarding its putative role in the two ABA responses described above. Abscisic acid has been reported to induce increases in cytoplasmic Ca^{2+} in a variety of cell types (*32*) and to arrest cell division preferentially in the G1 phase (*33*). In *Arabidopsis* root meristems ABI1 might, in response to applied ABA or ABA-induced Ca^{2+} changes, antagonize the various phosphorylation events required for the synthesis and activity of the $p34^{cdc2}$- and G1 cyclin-like complex controlling entry into S phase (*34*). Numerous lines of evidence support the idea that in guard cells Ca^{2+} acts as one of the intracellular second mes-

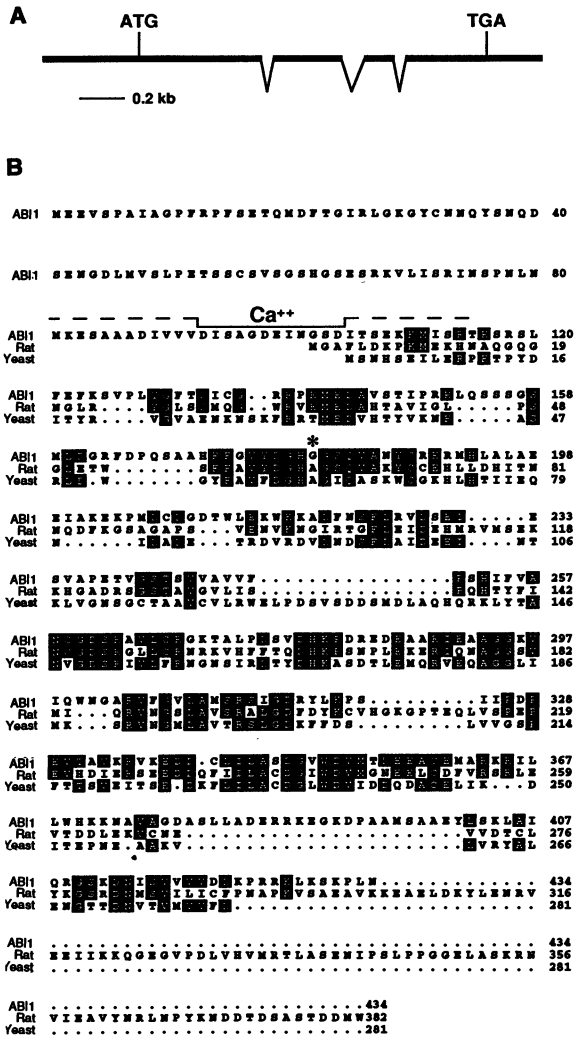

Fig. 4. (**A**) Structure of the *ABI1* gene. Exons are denoted by thick lines and introns are indicated by thin lines. The three introns contain 70, 131, and 92 nucleotides, respectively, from the 5′ to the 3′ end of the gene. Positions of the ATG and TGA codons delimiting the large open reading frame are indicated. The nucleotide sequence of the pcABI1-C38 cDNA has been deposited in the EMBL database (X77116). (**B**) The alignment of the ABI1 amino acid sequence with those of two representative members of the 2C class of protein phosphatases, for which enzymatic activities have been examined [rat (*29*), GenPept J04503, and yeast (*30*), GenPept L14593]. Alignment was produced by the GCG PileUp routine (*38*), with the use of a gap weight of 3.0 and a gap length weight of 0.1. Residues that are conserved between ABI1 and at least one of the PP2C sequences are displayed as reverse print. The ABI1 region with structural features of a calcium-binding EF hand is overlined with a plain line for the segment fitting the consensus sequence for the calcium-binding fold and with dashed lines for the flanking α helices. The *ABI1* coding region contains a non-silent nucleotide difference between the Col and Lan wild types, which converts Ile^{105} (Col) into Val (Lan). The *abi1-1* mutation is a G to an A transition at nucleotide 970 of the pcABI1-C38 cDNA insert, converting Gly^{180} (indicated by the asterisk) to Asp (*39*).

sengers involved in the ABA regulation of stomatal aperture (*3*, *32*). Moreover, stomatal opening as well as some of the electrogenic units involved (such as the plasma membrane H^+ pump and inward-rectifying K^+ channel) are sensitive to protein phosphorylation (*35*). The ABI1 protein could couple ABA stimulus to stomatal response by modifying the phosphorylation states of these target membrane proteins. Although the *abi1* mutant has so far been analyzed only with respect to ABA sensitivity, the molecular features of the ABI1 protein open the possibility that it may have a more versatile role. The ABI1 protein might serve as an exquisite cross talk element integrating ABA and other Ca^{2+}-dependent stimuli that converge on phosphorylation-regulated signaling pathways.

REFERENCES AND NOTES

1. A. M. Hetherington and R. S. Quatrano, *New Phytol.* **119**, 9 (1991).
2. J. A. D. Zeevaart and R. A. Creelman, *Annu. Rev. Plant Physiol. Plant Mol. Biol.* **39**, 439 (1988).
3. J. I. Schroeder, *Philos. Trans. R. Soc. London B* **338**, 83 (1992); M. R. Blatt and G. Thiel, *Annu. Rev. Plant Physiol. Plant Mol. Biol.* **44**, 543 (1993).
4. K. Skriver and J. Mundy, *Plant Cell* **2**, 503 (1990).
5. M. J. Guiltinan, W. R. Marcotte Jr, R. S. Quatrano, *Science* **250**, 267 (1990); K. Oeda, J. Salinas, N.-H. Chua, *EMBO J.* **10**, 1793 (1991).
6. C. Hornberg and E. W. Weiler, *Nature* **310**, 321 (1984).
7. D. R. McCarty *et al.*, *Cell* **66**, 895 (1991).
8. J. Giraudat *et al.*, *Plant Cell* **4**, 1251 (1992).
9. M. Koornneef, G. Reuling, C. M. Karssen, *Physiol. Plant.* **61**, 377 (1984). The *abi1-1* mutant, isolation number AII, was used throughout the present study.
10. R. R. Finkelstein and C. R. Somerville, *Plant Physiol.* **94**, 1172 (1990); J. A. Schnall and R. S. Quatrano, *ibid.* **100**, 216 (1992); N. Vartanian, L. Marcotte, J. Giraudat, *ibid.* **104**, 761 (1994).
11. S. J. Gilmour and M. F. Thomashow, *Plant Mol. Biol.* **17**, 1233 (1991); V. Lang and E. T. Palva, *ibid.* **20**, 951 (1992); K. Nordin, T. Vahala, E. T. Palva, *ibid.* **21**, 641 (1993); K. Yamaguchi-Shinozaki and K. Shinozaki, *Mol. Gen. Genet.* **236**, 331 (1993).
12. Surface-sterilized *Arabidopsis* seeds were placed on germination medium (*20*) agar plates with or without 10 μM ABA [mixed isomers (Sigma)]. These plates were then incubated in a growth chamber at 20°C with a 16-hour light (20,000 lux) photoperiod. For the analysis of cell division in root meristems, 6-day-old seedlings were placed in a 30 μM BrdU aqueous solution for 2 hours. Incorporated BrdU was detected in squashed root tips after a modified indirect immunofluorescent method based on the protocol of M. Levi, E. Sparvoli, S. Sgorbati, and D. Chiatante [*Physiol. Plant.* **79**, 231 (1990)]. After counterstaining with propidium iodide (2 μg/ml) for 10 min, slides were mounted in anti-fade solution (Citifluor, London) for examination under a Reichert (Buffalo, NY) epifluorescence microscope. The incorporation of BrdU was monitored in each genotype by examination of 10 root tips in each of three independent batches of seedlings.
13. M. Bouvier-Durand and J. Giraudat, unpublished results.
14. Stomatal apertures were measured on freshly excised rosette leaves (taken from the first pair of true leaves) from 3-week-old wild-type and *abi1-1* plantlets (*12*). Leaves were harvested in the middle of the light period, and stomata present on the abaxial surface were visualized under a microscope. Apertures were measured on all stomata (25 to 30) present in one field randomly selected in the median zone of each leaf examined (total of four leaves, each from distinct plantlets, per genotype). The mean aperture of *abi1-1* stomata was significantly ($P \leq 0.0005$; two-sample unpaired *t* test) higher than that in wild type.
15. B. M. Hauge *et al.*, *Plant J.* **3**, 745 (1993).
16. RFLP segregation analysis was performed (*8*) with the use of plants with recombination breakpoints either in the *cer2* to *abi1* interval (six recombinants) or in the *cer4* to *abi1* interval (16 recombinants). These recombinant plants were selected from F2 populations generated by the crossing of wild-type Columbia (Col) to either *cer2*, *abi1-1* or *cer4*, *abi1-1* digenic mutants in the Lan background. The markers tested were found to map in the order of m557-*cer2*-*abi1*-PG11-m272-g4513-g17340-*cer4*-*g3088*, which differs in the case of PG11 from the current integrated genetic and RFLP map of the *Arabidopsis* genome (*15*).
17. E. R. Ward and G. C. Jen, *Plant Mol. Biol.* **14**, 561 (1990); E. Grill and C. Somerville, *Mol. Gen. Genet.* **226**, 484 (1991).
18. For chromosome walking, ends corresponding to the *Arabidopsis* DNA insert in the YAC clones were isolated by inverse polymerase chain reaction (PCR) with the use of oligonucleotide primers specific to the vector arms or by plasmid rescue (*17*). The 13 overlapping YACs identified, in addition to the five clones depicted in Fig. 2A, are EG11F9 (rearranged), EG9E1, EW9C10, EG7G8, EG1F12 (rearranged), EG7H2 (rearranged), EW6D10, and EW18C4.
19. Pollen from the *abi1-1* mutant was used to fertilize a wild-type tetraploid Lan line. The resulting *abi1-1–ABI1–ABI1* triploid F1 progeny showed ABA-resistant root growth and reduced seed dormancy similar to the original homozygous *abi1-1–abi1-1* mutant.
20. D. Valvekens, M. Van Montagu, M. Van Lijsebettens, *Proc. Natl. Acad. Sci. U.S.A.* **85**, 5536 (1988).
21. The DNA inserts of isolated phages were released in intact form by cutting with appropriate restriction enzymes within the polylinker of λFIXII. After the ends were filled, the inserts were cloned by blunt-end ligation into the Sma I site of the binary plant transformation vector pDE1000 (Plant Genetics System, Brussels). In this vector, the inserts are not placed under the control of a foreign promoter; the plant genes contained in the inserts thus remain driven by their natural promoters. All constructs were propagated in the *Agrobacterium tumefaciens* strain C58C1Rif(pGV2260) [R. Deblaere *et al.*, *Nucleic Acids Res.* **13**, 4777 (1985)]. For each construct, the progeny of at least five independently derived transgenic plants were analyzed. Segregations of ABA or kanamycin (plant selection marker of the pDE1000 T-DNA vector) resistance in the T1 progeny were analyzed in 50 to 100 seeds each. Surface-sterilized seeds were placed on germination medium (*20*) agar plates with or without either 3 μM ABA or kanamycin (50

μg/ml). Except for dormancy assays, the plates were first placed for 4 days at 4°C in the dark. They were then incubated in a growth chamber at 24°C with a 16-hour light photoperiod.
22. Deletion derivatives were generated by partial digestion with Bam HI or Bam HI and Sma I in combination, religated, and transformed into *Escherichia coli*. Seventy-five Tn5 insertion mutants were generated [P. Putnoky *et al.*, *J. Bacteriol.* **172**, 5450 (1990)] and mapped in the ΔE insert; seven of these mutants were subsequently selected to confirm the identity of the *abi1-1* locus by functional assay.
23. J. Leung and J. Giraudat, unpublished results.
24. The pcABI1-C38 clone originates from a cDNA library constructed from *Arabidopsis* leaves (Col wild type). The full insert and isolated restriction fragments were subcloned into pBluescript KS+ (Stratagene) for sequence determination. Six overlapping fragments encompassing the transcribed region of the *ABI1* gene were amplified by PCR (with the use of specific primers) from Lan wild-type genomic DNA and from the *abi1-1* mutant DNA insert of λE4-1R2. The amplified fragments were subcloned into pBluescript KS+ for sequence determination. Nucleotide differences were verified from independently generated PCR products. Double-stranded plasmid DNA was sequenced on an Applied Biosystems (Foster City, CA) automated DNA sequencer (model 373A) with the use of dye primers as recommended by the manufacturer. Sequence analyses were done with programs of the Wisconsin GCG software package (*38*).
25. Database searches were performed at the U.S. National Center for Biotechnology Information with the use of the BLAST Network Service [S. F. Altschul, W. Gish, W. Miller, E. W. Myers, D. J. Lipman, *J. Mol. Biol.* **215**, 403 (1990)].
26. N. D. Moncrief, R. H. Kretsinger, M. Goodman, *J. Mol. Evol.* **30**, 522 (1990).
27. A. Bairoch, *Nucleic Acids Res.* **19**, 2241 (1991).
28. J. Garnier, D. Osguthorpe, B. Robson, *J. Mol. Biol.* **120**, 97 (1978).
29. S. Tamura *et al.*, *Proc. Natl. Acad. Sci. U.S.A.* **86**, 1796 (1989).
30. T. Maeda, A. Y. M. Tsai, H. Saito, *Mol. Cell. Biol.* **13**, 5408 (1993).
31. P. Cohen, *Annu. Rev. Biochem.* **58**, 453 (1989).
32. M. R. McAinsh, C. Brownlee, M. Sarsag, A. A. R. Webb, A. M. Hetherington, in *Abscisic Acid: Physiology and Biochemistry*, W. J. Davies and H. G. Jones, Eds. (Bios Scientific, Oxford, 1991), pp. 137–152; S. Gilroy, M. D. Fricker, N. D. Read, A. J. Trewavas, in *Progress in Plant Growth Regulation*, C. M. Karssen, L. C. van Loon, D. Vreugdenhil, Eds. (Kluwer Academic, Dordrecht, Netherlands, 1992), pp. 105–115.
33. M. Bouvier-Durand, M. Real, D. Côme, *Plant Physiol. Biochem.* **27**, 511 (1989); M. Levi, P. Brusa, D. Chiatante, E. Sparvoli, *In Vitro Cell. Dev. Biol.* **29P**, 47 (1993).
34. T. Jacobs, *Dev. Biol.* **153**, 1 (1992); C. Staiger and J. Doonan, *Curr. Opin. Cell Biol.* **5**, 226 (1993).
35. Y. Lee and S. M. Assmann, *Proc. Natl. Acad. Sci. U.S.A.* **88**, 2127 (1991); S. Luan, W. Li, F. Rusnak, S. M. Assmann, S. L. Schreiber, *ibid.* **90**, 2202 (1993).
36. Three independent C24 transgenic lines homozygous for the λE4-1R2 transgene were tested on nine concentrations of ABA ranging from 0 to 10 μM. Concentrations of 0.2 μM ABA inhibited root elongation (scored after 4 days) in 50% of the C24 wild-type seeds and of 0.5 μM ABA in 100% of the C24 wild-type seeds. In the transgenic lines, up to 3 μM ABA had no detectable effect, whereas 8 to 10 μM ABA was required to inhibit root development in 50% of the seeds. Freshly harvested mature seeds of these transgenic lines also displayed reduced dormancy because, in the absence of added ABA, 100% of the transgenic seeds germinated within 2 days, whereas only 5% of the C24 wild-type seeds had germinated after 2 days and 25% of the seeds had germinated after 7 days.
37. J. Leung, D. A. R. Sinclair, S. Hayashi, G. M. Tener, T. A. Grigliatti, *J. Mol. Biol.* **219**, 175 (1991).
38. J. Devereux, P. Haeberli, O. Smithies, *Nucleic Acids Res.* **12**, 387 (1984).
39. Single-letter abbreviations for the amino acid residues are as follows: A, Ala; C, Cys; D, Asp; E, Glu; F, Phe; G, Gly; H, His; I, Ile; K, Lys; L, Leu; M, Met; N, Asn; P, Pro; Q, Gln; R, Arg; S, Ser; T, Thr; V, Val; W, Trp; and Y, Tyr.
40. We thank H. M. Goodman for support during the early phase of this work; B. Hauge, H. M. Goodman, and E. M. Meyerowitz for RFLP probes; S. Brown, B. Labidi, and J.-R. Prat for advice on microscopy; T. Peeters and M. Koornneef for seed stocks and unpublished genetic mapping data; M.-O. Fauvarque for initial RFLP analysis; C. Somerville and E. Ward for YAC banks; A. Bent, D. Dahlbeck, T. Tai, B. Staskawicz, F. Katagiri, M. Mindrinos, F. Ausubel, A. Bachmair, and M. Kreis for cDNA libraries and purified clones; F. Parcy and C. Valon for RNA samples and blots; B. Hoffmann, G. Petrovics, and E. Kondorosi for materials and protocols on Tn5 mutagenesis; Plant Genetics Systems for the T-DNA vector pDE1000; R. Drouen for gardening work; and J. Guern, B. Gronenborn, S. Brown, U. Bonas, and J. Laufs for comments on the manuscript. Supported by the Centre National de la Recherche Scientifique, the European Economic Community BRIDGE program (BIOT-CT90-0207), and the Ministère de la Recherche et de la Technologie (91.T.0441).

3 February 1994; accepted 26 April 1994

A Protein Phosphatase 2C Involved in ABA Signal Transduction in *Arabidopsis thaliana*

Knut Meyer, Martin P. Leube, Erwin Grill*

The plant hormone abscisic acid (ABA) mediates various responses such as stomatal closure, the maintenance of seed dormancy, and the inhibition of plant growth. All three responses are affected in the ABA-insensitive mutant *abi1* of *Arabidopsis thaliana*, suggesting that an early step in the signaling of ABA is controlled by the *ABI1* locus. The *ABI1* gene was cloned by chromosome walking, and a missense mutation was identified in the structural gene of the *abi1* mutant. The *ABI1* gene encodes a protein with high similarity to protein serine or threonine phosphatases of type 2C with the novel feature of a putative Ca^{2+} binding site. Thus, the control of the phosphorylation state of cell signaling components by the *ABI1* product could mediate pleiotropic hormone responses.

The sesquiterpenoid plant hormone ABA is involved in many aspects of growth and development such as embryo development, seed dormancy, and adaptation responses toward low water potentials (*1*). Under conditions of water shortage, ABA induces the closure of leaf stomata and the formation of specific proteins involved in the desiccation response. The amount of ABA increases during water stress, and high concentrations of ABA inhibit plant growth.

Abscisic acid affects the expression of several genes involved in seed maturation and the desiccation response (*2*). The gene expression is modulated by ABA through a *cis*-acting regulatory element (*3*), for which a DNA binding factor has been identified (*4*). In maize and *Arabidopsis*, two structurally similar DNA binding proteins are involved in the control of seed maturation and dormancy (*5*). Individual components that act in the signaling cascade of ABA in the stomatal response are just beginning to emerge. Inositoltrisphosphate and Ca^{2+} can evoke stomatal closure (*6*), a process that requires the concerted regulation of at least four different ion channels, including channels for Ca^{2+} and anions as well as inward- and outward-rectifying K^+ channels (*7*). High-affinity binding sites for ABA at the cytoplasmic membrane of stomatal guard cells have been identified (*8*) but not further characterized.

The loci *ABI1* and *ABI2* of *Arabidopsis* are possible candidates for the encoding of an ABA perception site or early steps in its signal transduction (*9*). Mutants of both loci were found to be ABA-insensitive and revealed pleiotropic alterations in their responses toward ABA, whereas endogenous ABA levels and the catabolism of ABA were not affected. The dominant *ABI1* mutation is characterized by causing a wilty phenotype as well as ABA-insensitive seed germination and growth.

We are interested in elucidating the individual steps that lead to the control of plant growth by ABA. In this report, we describe the identification of the *Arabidopsis ABI1* gene. The gene encodes a product that has sequence homology with the class of protein serine or threonine phosphatase 2C. The ABI1 gene product has the additional features of a putative adenosine triphosphate (ATP) or guanosine triphosphate (GTP) binding site and an amino-terminal extension with a possible Ca^{2+} binding site.

The *ABI1* locus has been mapped to the chromosome 4 of *Arabidopsis* between the genetic markers *cer2* and *ap2* at a position

Institute of Plant Sciences, Swiss Federal Institute of Technology, Universitätsstrasse 2, 8092 Zürich, Switzerland.

*To whom correspondence should be addressed.